Correlation between pretreatment FDG-PET biological target volume and location of T-site failure after definitive radiation therapy for head and neck cancers

HELLA M. B. SAND[1], ANNE H. BRUNØ[2], LISBETH J. ANDERSEN[2] & JESPER CARL[1]

[1]*Department of Medical Physics, Oncology, Aalborg University Hospital, Aalborg, Denmark and* [2]*Department of Oncology, Aalborg University Hospital, Aalborg, Denmark*

To the Editor,

Head and neck squamous cell carcinoma accounts for approximately 5% of malignancies worldwide [1]. It is predominantly a loco-regional disease, which is accessible to curative intent treatment with surgery and/or radiation therapy (RT) [2,3]. Traditionally target-volume delineation in head and neck cancer (HNC) has been based on anatomic data supplied by physical examination and computed tomography (CT) [1,4]. In recent years, positron emission tomography (PET) using the tracer ^{18}F-fluorodeoxyglucose (FDG) has become an important diagnostic tool for evaluation of HNC and is applied in various clinical settings including RT treatment planning in which it is used as complementary information to the conventional methods [5].

PET/computed tomography (CT) incorporates metabolic tumor function with anatomic localization with several potential advances [6]. Studies conclude that FDG-PET/CT is more accurate than conventional staging in HNC [7,8] and FDG-PET/CT detects primary HNC with high sensitivity (> 95%) [9]. PET-defined target volumes may be an area that warrants intensive therapy in order to improve failure rates and outcomes in HNC. Two prototypical strategies have been considered in the literature: *sub-volume boosting*, which involves a selection of a "target within the target", defined by image segmentation on the basis of quantitative information in the image, or *dose painting by numbers*, which is a voxel-level prescription that maps a range of image intensities onto a range of doses [10].

During the past years, a number of studies have found that the majority of HNC failures map to the pretreatment PET abnormality. Soto et al. [11] found that 8/9 (89%) loco-regional failures were within the pretreatment PET-volume while La et al. [12] found 6/7 (86%) local failures within the pretreatment PET-volume and only the one regional failure to occur outside the pretreatment PET-volume. Madani et al. [13] also reported the majority of the local relapses to occur inside the PET-avid region or at its borders [5/9 (56%)]. These observations suggest that FDG might be a useful tracer for detecting intratumor regions of increased radiation resistance. In continuation of the findings in these studies, we hypothesize that failures of HNC arise from the PET avid volume and possibly from the areas of the PET volume with the strongest FDG-signal.

Material and methods

Patients

HNC patients definitively treated with intensity-modulated radiation therapy (IMRT) at the Department of Oncology at Aalborg University Hospital were included in this study. Between January 2007 and December 2013, 31 patients with squamous cell HNC treated with single-modality RT were found to have an available in house pretreatment FDG-PET scan and an in house FDG-PET scan visualizing a loco-regional infield recurrence. We excluded patients with singular N-site or M-site failure and focused our study on the 19 patients with a loco-regional T-site failure. Two patients were afterwards excluded due to technical difficulties, as they were positioned very differently on the two scans resulting in bad scanning co-registrations leaving a final study group of 17 patients. Details of patient and tumor characteristics are provided in Table I.

Image acquisition

In the study group, the pre-treatment FDG-PET/CT scan was obtained either with the purpose of RT planning or as part of the clinical staging proce-

Correspondence: H. Sand, Department of Medical Physics, Oncology, Aalborg University Hospital, Hobrovej 18-22, 9000 Aalborg, Denmark. Tel: + 45 97661584. E-mail: hmbs@rn.dk

(Received 5 June 2015; accepted 2 July 2015)

ISSN 0284-186X print/ISSN 1651-226X online © 2015 Informa Healthcare
DOI: 10.3109/0284186X.2015.1071919

dure. In cases where the pretreatment FDG-PET/CT scan was a diagnostic scan, a separate CT scan had been used for planning. Otherwise the pretreatment FDG-PET/CT had been used for planning. PET/CT imaging was performed on a Discovery RT following standardized procedures. After intravenous injection of FDG, patients were resting for about 60 minutes to avoid muscular FDG uptake. Subsequently patients were scanned. The scanning volumes were covering from the top of the skull to the level of the arcus aorta.

The original gross tumor volume

On the therapy CT images manual delineation of the gross tumor volume (GTV), the clinical target volume (CTV) and the planning target volume (PTV) was originally performed according to current clinical guidelines as outlined by the Danish Head and Neck Cancer Study Group (DAHANCA) [14]. The original GTV was thus delineated by using all available diagnostic imaging present as well as the results of the physical examination. As the focus of this study is primary head and neck tumors, all N-sites included in the original GTV, except from possible lymph node conglomerates confluent with the T-site, were erased. This corrected GTV called GTV_pre was then transferred to the recurrence FDG-PET scan by means of deformable co-registration of the pretreatment and recurrence PET/CT scans in the Eclipse treatment planning system from Varian.

FDG-PET-based target volumes

Furthermore, we delineated the primary tumor on the pretreatment PET and the T-site failure on the recurrence PET by means of a 41% fixed threshold of the maximum signal intensity value measured in counts (Mbq/ml) corrected for the background activity and called these volumes GTV41_pre and GTV41_fail. We chose a threshold level of 41% of the background-subtracted signal, as this value was found to correspond the best to the physical diameter of different cylindrical sources with FDG-activity in a phantom study using FDG-PET scanning for automatic delineation conducted by Davis et al. [15]. An example of delineation is shown in Figure 1.

The maximum intensity signal was defined as the hottest voxel in the primary tumor. The mean background activity was obtained as a mean value from nine adjacent voxels in a manually defined region in the left neck musculature far away from the primary tumor and any metastatic lymph nodes. The maximum standadized uptake value (max SUV), an index of glucose metabolism, which equals the FDG uptake in the hottest voxel in tumor tissues normalized by the injected dose and body weight [6], was calculated manually from information about the injected tracer dose, the patients weight on the day of the scan and the value of the hottest voxel in the tumor.

In several cases, evident physiological FDG-uptake was included in the autosegmented volume, including the physiological brain activity, swallowing activity in the muscles of the mouth or throat and brown adipose tissue. Moreover, possible

Table I. Details of patient and tumor characteristics.

Patient	TNM	Tumor site	GTV_pre (cm^3)	GTV41_pre (cm^3)	GTV41_fail (cm^3)
1	T1N0M0	Larynx	5.24	2.01	9.72
2	T4N2M0	Oral cavity	42.48	18.43	30.94
3	T1N3M0	Oropharynx	3.47	1.01	10.52
4	T2N1M0	Tonsil	9.72	3.91	7.25
5	T4N2M0	Rhinopharynx	26.15	4.42	8.12
6	T4N1M0	Oral cavity	98.03	6.23	4.51
7	T2N0M0	Larynx	0.86	2.19	6.76
8	T1N0M0	Tonsil	10.31	4.68	9.01
9	T4N1M0	Oral cavity	28.82	12.8	15.91
10	T2N2M0	Hypopharynx	9.01	2.87	1.83
11	T3N1M0	Oral cavity	8.81	11.19	11.33
12	T4N2M0	Hypopharynx	75.6	36.34	18.96
13	T4N2M0	Larynx	42.72	20.24	25.62
14	T2N2M0	Oropharynx	7.61	1.22	3.27
15	T4N1M0	Rhinopharynx	32.5	13.06	6.76
16	T1N0M0	Larynx	0.47	2.86	7.27
17	T2N2M0	Oropharynx	7.55	2.51	20.16

Tumor and patient characteristics of 17 HNC patients together with the volumes of the GTV manually delineated on a pretreatment FDG-PET/CT scan (GTV_pre) and automatically delineated on a pretreatment and recurrence PET-scan from a 41% threshold of the maximum signal intensity corrected for the background (GTV41_pre and GTV41_fail).

autosegmented metastatic lymph nodes were of no interest in this study. These structures were therefore manually erased in consensus with an experienced oncologist.

In two cases in which a lymph node conglomerate was confluent with the primary tumor with no distinct boundary, we chose to include the lymph node conglomerate in our autosegmented volume. In two cases of rhinopharyngeal carcinoma with invasion of the cerebrum, we chose to exclude the tumor involvement of the brain tissue as outlined by the original automatic GTV, as the possible malignant FDG-PET signal from this area was unseperable from the normal FDG activity of the brain. We did not exclude air cavities, such as, i.e. the trachea in our GTV41-delineation, when the tumor was located in close proximity without any clear border.

Data analysis

The overlapping volumes of the pretreatment volumes and the failure volume were delineated automatically by means of the Boolean tool in Eclipse resulting in two new volumes; 'GTV_pre ∩ GTV41_fail' and 'GTV41_pre ∩ GTV41_fail'.

Results

The median GTV_pre was 9.72 cm^3 (0.47–98.03 cm^3), while the median GTV41_pre was 4.42 cm^3 (1.01–36.34 cm^3). The GTV_pre was in all cases but three substantially greater than the GTV41_pre. Two of three cases with larger GTV41_pre than GTV_pre were small tumors of the supraglottic region, in which air in the trachea, which was not excluded from the autosegmentation, was accountable of the overestimation of the tumor volume on PET (Patient 7 and 16 in Table I). The last case was a relatively large tongue cancer stage T3, which measured 8.81 cm^3 on GTV_pre and 11.19 cm^3 on GTV41_pre (Patient 11 in Table I).

In total 17/17 failures were located inside the PET volume defined as the GTV41_fail. The median GTV41_fail was 9.01 cm^3 (1.83–30.94 cm^3). The median 'GTV_pre ∩ GTV41_fail' was 3.15 cm^3 (0.08–12.75 cm^3), while the median 'GTV41_pre ∩ GTV41_fail' was 1.51 cm^3 (0–7.27 cm^3). The overlap volumes for each patient are plotted in Figure 2.

We also tried to delineate the primary tumor with a 60% (GTV60_pre) and 80% (GTV80_pre) threshold of the maximum signal intensity value subtracted from the background and then found 15/17 (88%) for the GTV60_pre and 8/17 (47%) for the GTV80_pre to overlap with the volume GTV41_fail. It was obvious though that the low spatial resolution of the software program Eclipse and the PET scan made these small volumes very vulnerable to errors, and therefore we did not analyze these data further.

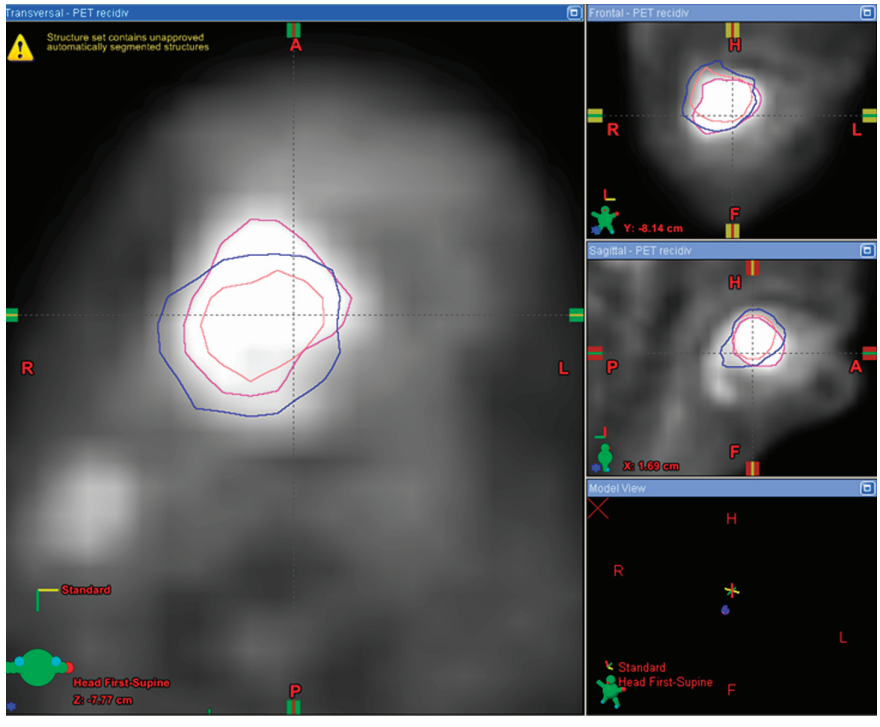

Figure 1. Delineations on Patient 9 shown in transversal, axial and sagittal view. Blue line is the GTV_pre, orange line is the GTV41_pre and purple line is the GTV41_fail.

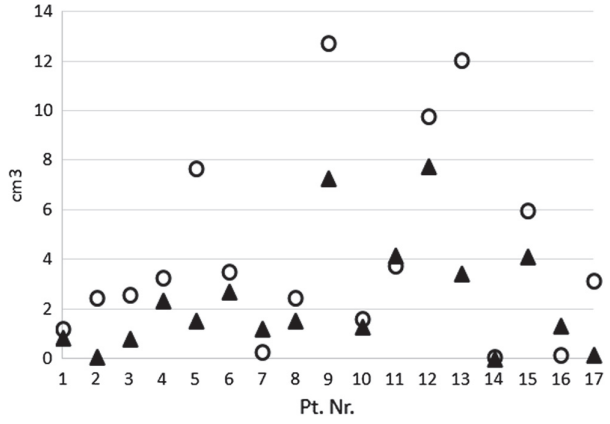

Figure 2. Overlap volumes in cm^3 for all patients. Circles: GTV_pre ∩ GTV41_fail. Triangles: GTV41_pre ∩ GTV41_fail.

Discussion

In the present study 17 patients had a FDG-PET/CT-scan of both the primary tumor and the T-site recurrence after curative RT. This gave us the opportunity to analyze on an automatic and hence user independent delineation of the GTV on both scans. The two scans were linked together by deformable co-registration. In all 17 patients an overlap existed between the PET-active volume on the planning and recurrence scan, which indicates a high probability of the recurrence to originate from the PET-active volume identified on the planning PET/CT.

Treatment outcome in HNC remains heterogeneous. Therefore still more focus have been on the identification of novel biologic parameters with the goal of developing individualized treatment strategies for these patients. Detailed patterns of failure studies may help determine possible targets for dose-escalation with RT, which could lead to increased loco-regional control. The ideal map of therapeutic efficacy from a pattern of failure study would be a map of the probability of failing in specific sub-regions of the target, which can be derived prior to RT. This could lead to a non-uniform radiation dose distribution to the target volume by dose-escalation to these sub-regions. In this study FDG-PET has been used as a tool for mapping these sub-regions. Our study indicates, even though not conclusive, that the recurrence may come from the sub-volume with the strongest FDG-signal. This observation is in accordance with other recent studies suggesting that most recurrences occur in the FDG-PET positive area of the primary tumor [13,16].

One of the question left is the exact value of which escalated dose is required to obtain local control of disease in the PET active volumes.

Declaration of interest: The authors report no conflicts of interest. The authors alone are responsible for the content and writing of the paper.

References

[1] Vernon MR, Maheshwari M, Schultz CJ, Michel MA, Wong SJ, Campbell BH, et al. Clinical outcomes of patients receiving integrated PET/CT-guided radiotherapy for head and neck carcinoma. Int J Radiat Oncol Biol Phys 2008;70:678–84.

[2] Overgaard J, Sand Hansen H, Jørgensen K, Hansen MH. Primary radiotherapy of larynx and pharynx carcinoma: An analysis of factors influencing local control and survival. Int J Radiat Oncol Biol Phys 1986;12:515–21.

[3] Overgaard J, Sand Hansen H, Specht L, Overgaard M, Grau C, Andersen E, et al. Five compared with six fractions per week of conventional radiotherapy of squamous-cell carcinoma of head and neck: DAHANCA 6 & 7 randomised controlled trial. Lancet 2003;362:933–40.

[4] Castaldi P, Leccisotti L, Bussu F, Micciche F, Rufini V. Role of 18F-FDG PET-CT in head and neck squamous cell carcinoma. Acta Othorhinolaryngol Ital 2013;33:1–8.

[5] Riegel AC, Berson AM, Destian S, Ng T, Tena LB, Mitnick RJ, et al. Variability of gross tumor volume delineation in head-and-neck cancer using CT and PET/CT fusion. Int J Radiat Oncol Biol Phys 2006;65:726–32.

[6] Nestle U, Weber W, Hentschel M, Grosu AL. Biological imaging in radiation therapy: Role of positron emission tomography. Phys Med Biol 2009;54:R1–25.

[7] Czernin J, Allen-Auerbach M, Schelbert HR. Improvements in cancer staging with PET/CT: Literature-based evidence as of September 2006. J Nucl Med 2007;48:78S–88S.

[8] Connell CA, Corry J, Milner AD, Hogg A, Hicks RJ, Rischin D, et al. Clinical impact of, and prognostic stratification by, F-18 FDG PET/CT in head and neck mucosal squamous cell carcinoma. Head Neck 2007;29:986–95.

[9] Roh JL, Yeo NK, Kim JS, Lee JH, Cho KJ, Choi SH, et al. Utility if 2-[18F] fluoro-2-deoxy-Dglucose positron emission tomography and positron emission tomography/computed tomography imaging in the preoperative staging of head and neck squamous cell carcinoma. Oral Oncol 2007;43:887–93.

[10] Betzen S, Gregoire V. Molecular-imaging-based dose painting – a novel paradigm for radiation therapy prescription. Semin Radiat Oncol 2011;21:101–10.

[11] Soto DE, Kessler ML, Piert M, Eisbruch A. Correlation between pretreatment FDG-PET biological target volume and anatomical location of failure after radiation therapy for head and neck cancers. Radiother Oncol 2008;89:13–8.

[12] La TH, Filion EJ, Turnbull BB, Chu JN, Lee P, Nguyen K, et al. Metabolic tumor volume predicts for recurrence and death in head-and-neck cancer. Int J Radiat Oncol Biol Phys 2009;74:1335–41.

[13] Madani I, Duthoy W, Derie C, Gersem WD, Boterberg T, Saerens M, et al. Positron emission tomography-guided, focal-dose escalation using intensity-modulated radiotherapy for head and neck cancer. Int J Radiat Oncol Biol Phys 2007;68:126–35.

[14] Grau K, editor. Retningslinjer for strålebehandling i DAHANCA 2004, 3rd ed [Internet]. DAHANCA, 2004 [Updated 2012 Dec 10]. https://www.dahanca.oncology.dk/uploads/Straaleforskrift2004.pdf

[15] Davis J, Reiner B, Huser M, Burger C, Szekely G, Ciernik I. Assessment of ^{18}F PET signals for automatic target volume definition in radiotherapy treatment planning. Radiother Oncol 2006;80:43–50.

[16] Due AK, Vogelius IR, Aznar MC, Bentzen SM, Berthelsen AK, Korreman SS, et al. Recurrences after intensity modulated radiotherapy for head and neck squamous cell carcinoma more likely to originate from regions with high baseline [18F]-FDG uptake. Radiother Oncol 2014;111:360–5.